

---

# The effect of finite accuracy in the manufacturing of Large Aperture Scintillometers

A.F. Moene, W.M.L. Meijninger, O.K. Hartogensis, B.G. Heusinkveld, and H.A.R. de Bruin

January 2005

Internal report 2005/1

Meteorology and Air Quality Group  
Wageningen University  
Duivendaal 2  
6701 AP Wageningen  
The Netherlands  
<http://www.met.wau.nl>

This work has been sponsored by the  
Dutch Technology Foundation STW  
(WMO4133)

---

# Contents

<b>1</b>	<b>Introduction</b>	<b>2</b>
<b>2</b>	<b>Alignment of mirrors in transmitter and receiver</b>	<b>3</b>
2.1	Ray geometry of spherical mirrors for a point source . . . . .	3
2.2	Finite size of the transmitting LED . . . . .	5
2.3	Path length and LED size . . . . .	8
<b>3</b>	<b>Settings of the electronics</b>	<b>10</b>
3.1	Signal processing: equations . . . . .	10
3.2	Signal processing: electronics . . . . .	11
3.3	Calibration of log-amplifiers in receiver . . . . .	13
3.3.1	Calibration procedure . . . . .	13
3.3.2	Error estimate . . . . .	13
3.4	Path setting on receiver . . . . .	14
3.4.1	Calibration procedure . . . . .	14
3.4.2	Error estimate . . . . .	14
3.5	Calibration of internal data logger . . . . .	15
3.5.1	Procedure . . . . .	15
3.5.2	Error estimate . . . . .	16
3.6	Error sources not addressed here . . . . .	16

---

# 1

## Introduction

This document deals with a number of aspects of the accuracy of the Dept. of Meteorology Large Aperture Scintillometers (LAS). Section 2 deals with the optical parts of the LAS. Section 3 discusses the effect on the accuracy of various settings in the electronics.

---

# 2

## Alignment of mirrors in transmitter and receiver

As far as the transmitter and receiver are concerned, the theory of the LAS is based on the assumption that both transmitter and receiver consist of a collection of point sources and point receivers, respectively. The point sources must be incoherent in phase.

In the LAS of Dept. of Meteorology the spherical mirrors of transmitter and receiver are supposed to represent such collection of point sources and point receivers. The actual transmitter is a LED placed in the focal point of the transmitter mirror. The actual receiver is a diode located in the focal point of the receiver mirror.

From an optical point of view the transmitter and receiver are identical (except for the size and shape of the transmitting LES and the receiving diode). Therefore, only the transmitter side of the optical configuration will be dealt with.

An ideal point source emits light in all directions with an intensity that is independent of direction. In this section it will be investigated how well this ideal is approximated by the current configuration of the LAS of Dept. of Meteorology. Three things have to be taken into account in this analysis <sup>1</sup>:

- The focal point of a spherical mirror depends on the distance from the optical axis of the reflecting point on the mirror;
- The emitting LED has a finite size;
- The distance between transmitter mirror and the receiver mirror determines the effect of the varying focal length of a spherical mirror.

### 2.1 Ray geometry of spherical mirrors for a point source

The LAS used by Dept. of Meteorology uses a LED placed in the focal point of a spherical mirror to produce a parallel beam. In this section the geometry of the beam produced by the transmitter and captured by the receiver will be investigated. Figure 2.1 shows the geometry of a beam originating from a point on the optical axis at a given distance from the mirror for a spherical mirror. For paraxial rays<sup>2</sup> the relationship between the radius of curvature of a mirror and the focal length is rather simple:

$$f = -\frac{R}{2} \tag{2.1}$$

where  $R$  is the radius of curvature which is negative for a concave mirror and positive for a convex mirror.

If the rays can no longer be assumed to be paraxial, the real focal point of a spherical mirror becomes dependent on the angle between the ray and the optical axis ( $\theta$ ). In order to find the focal length one has to return to the original definition of the focal point: the image distance for an object that is at an infinite distance from the mirror. Thus the ray originating from the object is parallel to the optical axis and crosses—after reflection by the mirror—the optical axis in the focal point. In figure 2.1 this would imply that  $\alpha = \phi$ . In order to determine the dependence of the focal length on the radial position of the point where the ray hits the mirror, the following relationships can be used:

$$f = x_2 + y_1 \tan \psi, \tag{2.2}$$

---

<sup>1</sup>The analysis in the forthcoming sections is based on the assumption of axisymmetry around the optical axis.

<sup>2</sup>Rays for which the angles with the optical axis are small enough to permit setting cosines equal to unity and the sines and tangents equal to the angles (Jenkins and White, 1976)

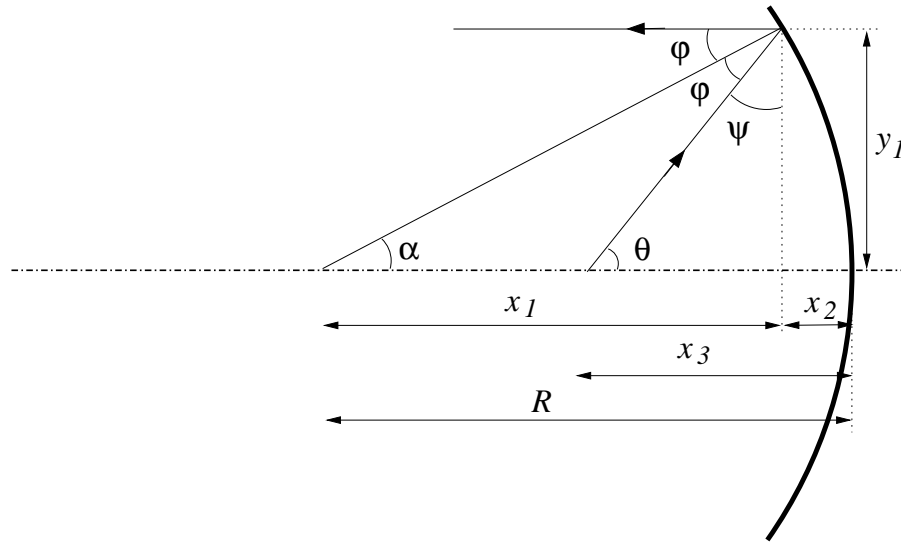


**Figure 2.1:** Spherical mirror: relationship between radius of curvature ( $R$ ), the distance of the point source to the mirror ( $x_3$ ) and the direction of a beam originating from that source.

where

$$x_1 = \sqrt{R^2 - y_1^2}$$

$$x_2 = R - x_1$$

$$\psi = \frac{1}{2}\pi - 2\phi = \frac{1}{2}\pi - 2 \arctan \frac{y_1}{x_1}$$

Figure 2.2 shows the deviation of the actual focal length from the nominal focal length as a function of the radial position of the incoming ray for the mirror used in the LAS of Dept. of Meteorology. It can be seen that at the edges of the mirror the deviation is 2.5 mm or less than 1%. The variation of the focal length can also be viewed in a different perspective: rays that originate from a given point on the optical axis of the mirror leave the mirror under different angles. In order to determine the angle ( $\eta$ ) between the optical axis and a ray originating from a given point on the optical axis (at a distance  $x_3$  from the mirror), the following relationships can be used.

$$\eta = 2\phi + \psi - \frac{1}{2}\pi, \quad (2.3)$$

where

$$\psi = \frac{1}{2}\pi - \theta = \frac{1}{2}\pi - \arctan \frac{y_1}{x_3 - x_2}$$

$$\phi = \frac{1}{2}\pi - \alpha - \psi$$

$$\alpha = \arctan \frac{y_1}{x_1},$$

so

$$\eta(y_1) = -2 \arctan \frac{y_1}{x_1} + \arctan \frac{y_1}{x_3 - x_2}. \quad (2.4)$$

In figure 2.3 the angle  $\eta$  is shown as a function of the radial position on the mirror where the ray is reflected (here  $x_3 = f$  and the parameters of the mirror are those of the spherical mirrors used in the LAS of Dept. of Meteorology). Indeed it can be seen that the ray is converging. The maximum deviation occurs

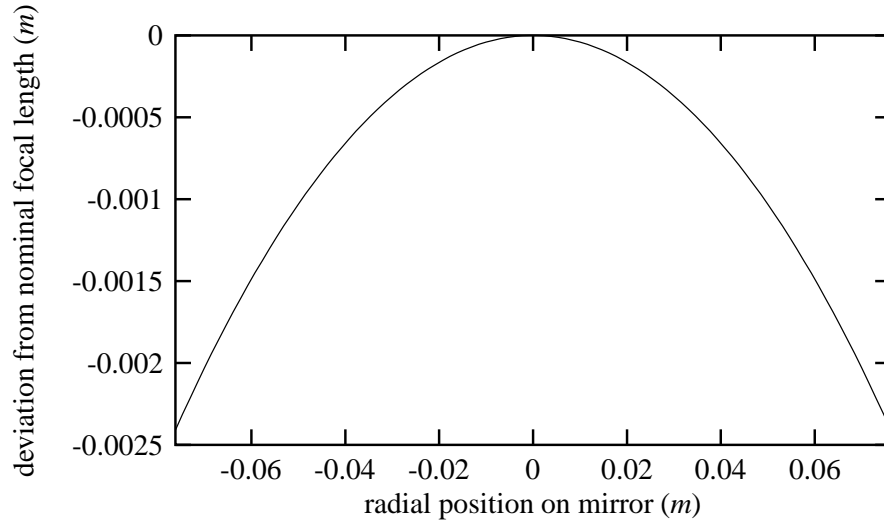


**Figure 2.2:** The deviation of the actual focal length from the nominal focal length as a function of the radial position of the incoming ray for a spherical mirror with focal length of 0.3048 m and a diameter of 0.1524 m.

at the edges and is of the order of  $0.1^\circ$ . In order to judge the effect of this deviation on the beam of the LAS, the displacement of a ray is given for a distance (measured parallel to the optical axis) of 1000 m in figure 2.4. For the outer edges of the mirror the displacement is about 2 m so that the total beam diameter has grown from 0.15 m at the transmitter to 4 m at the given position. This represents a considerable loss in radiative flux density, since the same amount of energy is spread over an area that is 700 times as large.

## 2.2 Finite size of the transmitting LED

The LED used in the transmitter has a diameter of 1.83 mm. This implies that the transmitter mirror is illuminated not by a point source but by a collection of point sources. As a consequence, each point on the mirror receives light from different sources. This is sketched in figure 2.5 (where the LED has been depicted as a plane source). In order to determine the half angle  $\gamma$  of the cone of light originating from the point of the we first determine the dependence of  $\eta$  on a displacement of the points source normal to the optical axis ( $y_3$ ):

$$\eta(y_1, y_3) = -2 \arctan \frac{y_1}{x_1} + \arctan \frac{y_1 - y_3}{x_3 - x_2}. \quad (2.5)$$

Then, for  $\gamma$  we find:

$$\gamma = \eta(y_1, 0) - \eta(y_1, y_3) \quad (2.6)$$

Figure 2.6 shows  $\gamma$  for two positions of the LED and a radius of the LED of 1 mm. The half-angle of the cone is only slightly dependent on the position on the mirror and the position of the LED on the optical axis ( $x_3$ ). The result shown is for positive values of  $y_3$ . The value of  $\gamma$  for negative  $y_3$  is —apart from its sign— nearly identical to that for  $y_3 > 0$  (within 0.0005 degrees).

A point source would emit light in all directions, whereas the points of the mirror reflect light in a limited cone only. However, if this cone illuminates the entire region of interest (i.e. the receiver mirror), the transmitter mirror can indeed be interpreted as a collection of points source. Whether the receiver mirror is completely illuminated depends on the distance between the two mirrors (see next section).

The points on the transmitter mirror behave like point sources in the sense that they emit light in all —relevant— directions. However, these rays are mutually incoherent, since they originate from different points on the surface of the LED. This implies that the point sources do *not* emit a spherical wave. Only with respect to the intensity are these points point sources (intensity is proportional to  $r^{-2}$ , where  $r$  is the distance from the source).

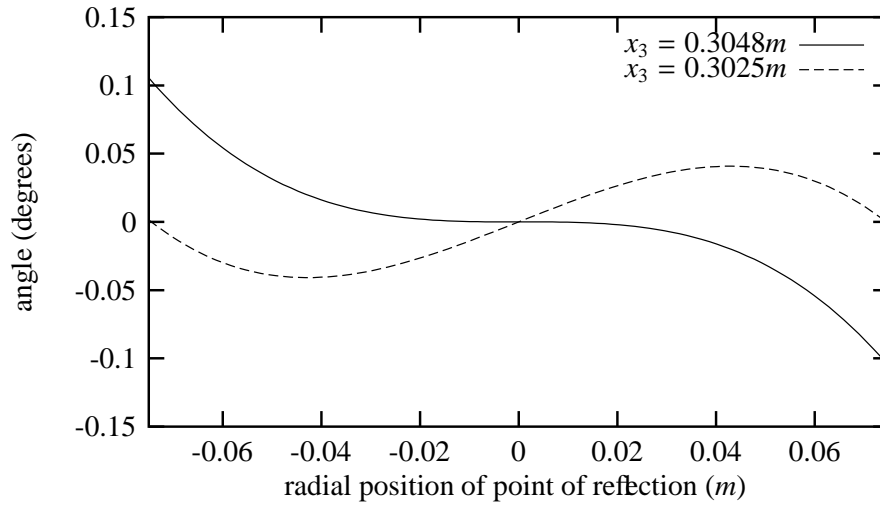


**Figure 2.3:** The angle of a rays originating from different points on the optical axis of a spherical mirror as a function of the radial position of the point of reflection on the mirror. Data are for a spherical mirror with focal length of  $0.3048\text{ m}$  and a diameter of  $0.1524\text{ m}$ .

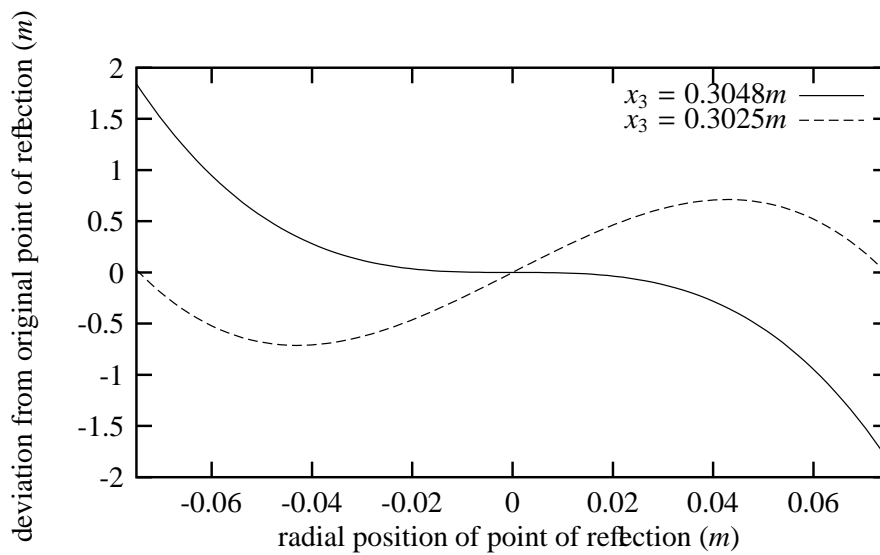


**Figure 2.4:** Deviation from its original radial position at the transmitter mirror of rays that originate from the different points on the optical axis of a spherical mirror. Deviation given as a function of the radial position of the point of reflection on the mirror. Data are for a spherical mirror with a focal length of  $0.3048\text{ m}$  and a diameter of  $0.1524\text{ m}$  at a distance of  $1000\text{ m}$  from the transmitter mirror.

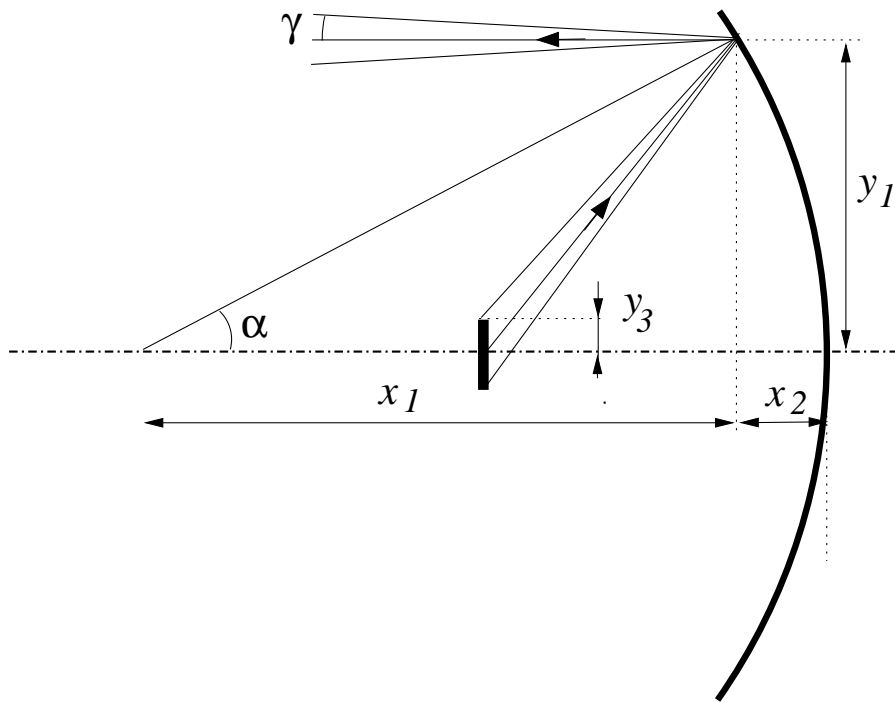


**Figure 2.5:** Spherical mirror: illumination of a mirror by a source of finite size gives relationship between radius of curvature ( $R$ ), the distance of the point source to the mirror ( $x_3$ ) and the direction of a beam originating from that source.

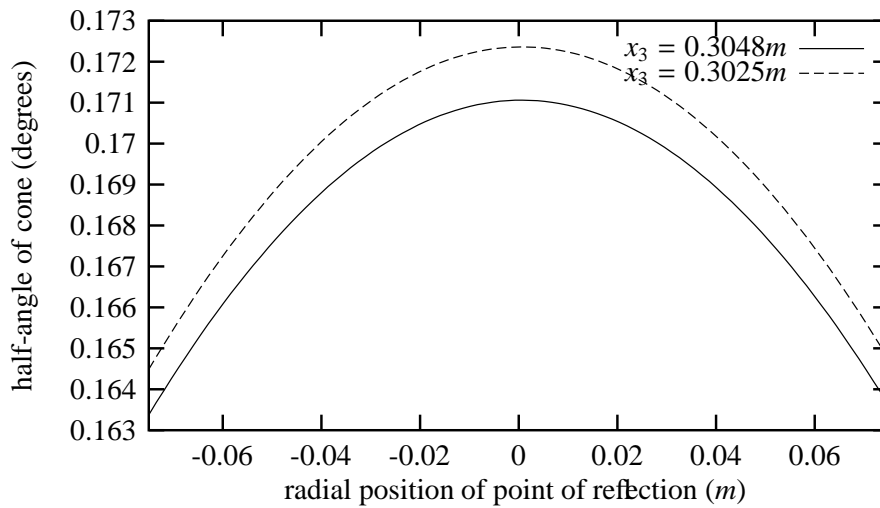


**Figure 2.6:** Half angle of the cone produced by a LED with a radius of  $0.91mm$  which illuminates a spherical mirror. The result for two positions of the LED are shown. Data are for a spherical mirror with a focal length of  $0.3048m$  and a diameter of  $0.1524m$



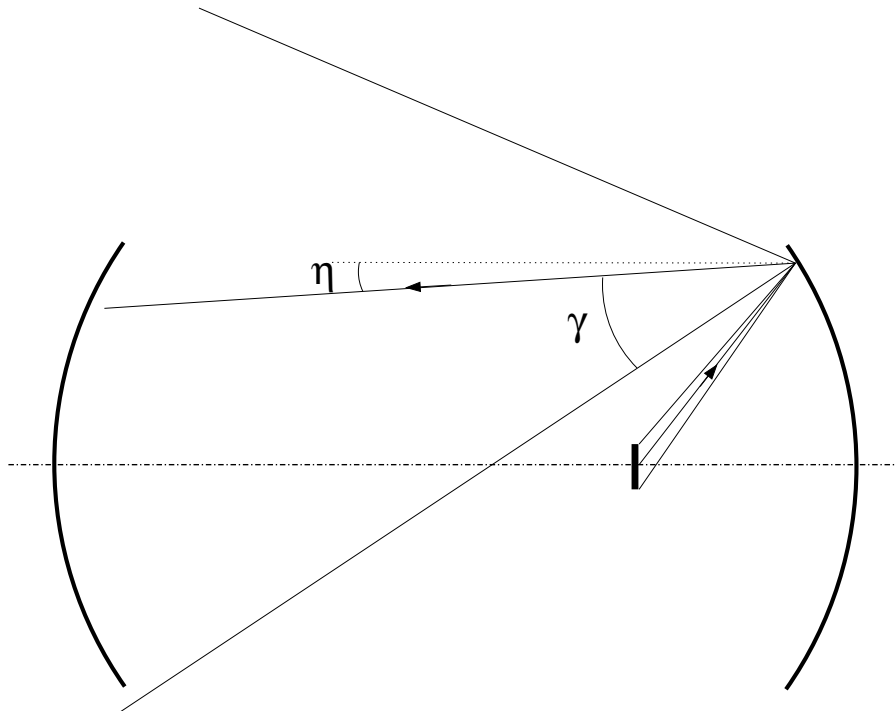


**Figure 2.7:** The cone of light originating from a LED at the nominal focal point of a spherical mirror (transmitter mirror at the right). Whether this cone illuminates the entire receiving mirror (left) depends on the angle of central ray ( $\eta$ ) and the half angle of the cone ( $\gamma$ ). Note that the conditions in equation 2.7 do not require that the central ray, drawn in this figure, hits the receiver mirror at all.

### 2.3 Path length and LED size

In order for each point on the transmitting mirror to act as a point source seen by the receiving mirror, the cone of light originating from that point should illuminate the entire receiver mirror (see also figure 2.7). This implies that:

$$L \geq (\text{sign } \eta \frac{1}{2} D - y_1) / \tan \eta(y_1, y_3) \quad (2.7)$$

For the configuration under consideration it can be anticipated that these conditions will be fulfilled: the maximum angle of a ray originating from the optical axis is of the order of 0.1 degrees (figure 2.3), whereas the half angle of the cone is of the order of 0.2 degrees (figure 2.6). Thus, for any point on the transmitter mirror, there are both rays that are directed towards the optical axis and rays that are directed outward ( $\eta + \gamma > 0$  and  $\eta - \gamma < 0$ ). This will ensure that a plane exists where the cone illuminates a region larger than the receiver mirror (i.e. larger than anything, given sufficient path length). Figure 2.8 illustrates the minimum path length required to fulfill these conditions of (2.7). It can be seen that the minimum path length is of the order of 35 to 55 m for the given configuration. With decreasing size of the LED, this minimum path length increases (since the half angle of the cone decreases). There will be a LED size, where the half angle of the cone will be less than  $\eta$ . In that case it is no longer ensured that the cone will illuminate the entire receiver mirror. For an axial position of the LED of  $x_3 = 0.3048m$  this point is reached at a LED radius of about 0.6 mm. For  $x_3 = 0.3025$  the minimum LED radius is about 0.25mm

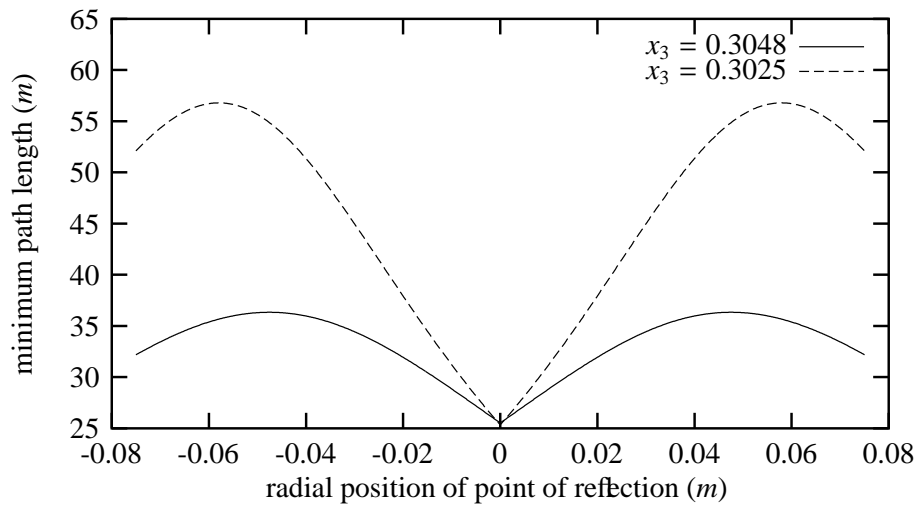


**Figure 2.8:** The minimum path length required to ensure that the cone of light originating from a given point on the transmitter mirror illuminates the entire receiver mirror. The cone is produced by a LED with a radius of  $0.91\text{mm}$  which illuminates a spherical mirror. The result for two positions of the LED ( $x_3$ ) are shown. Data are for a spherical mirror with a focal length of  $0.3048\text{ m}$  and a diameter of  $0.1524\text{ m}$

---

# 3

## Settings of the electronics

The light that is captured by the receiver is converted to a voltage by a diode detector. This voltage is converted in a number of steps to finally yield a signal that is related to  $C_{n^2}$ . Section 3.1 gives the equations that describe a number of conversions applied to the detector signal (the demodulation is *not* dealt with). Section 3.2 deals with the implementation those conversions in the electronics. Section 3.3 describes the procedure for the calibration of the log-amplifiers in the electronics, as well as the attainable accuracy. Section 3.4 describes the calibration of the path setting amplifier and finally section 3.5 deals with the calibration of the internal data logger.

### 3.1 Signal processing: equations

The electronics of the scintillometer have been designed in such a way that the output voltage is directly related to  $C_{n^2}$ :

$$V_{out} = {}^{10}\log C_{n^2} + 12 , \quad (3.1)$$

or

$$V_{out} = {}^{10}\log(C_{n^2} 10^{12}) . \quad (3.2)$$

According to Wang *et al.* (1978) :

$$\sigma^2(\ln(I)) = 0.892D^{-7/3}L^3C_{n^2} , \quad (3.3)$$

or equivalently,

$$C_{n^2} = 1.12D^{7/3}L^{-3}\sigma^2(\ln(I)) , \quad (3.4)$$

where  $I$  is the light intensity (to which the signal from the detector is proportional),  $D$  is the diameter of the beam and  $L$  is the path length.

The conversion of  $I$  to  $\ln(I)$  is done with a log-amplifier that gives an output of 2V per decade:  $2 \log(I)$ . Thus, to obtain  $\ln(I)$  one needs to convert the output signal (which is the input of the path setting amplifier) of the log-amplifier as:

$$\ln(I) = \frac{1}{2} \ln(10)(2 \log(I)) , \quad (3.5)$$

so

$$C_{n^2} = 1.12D^{7/3}L^{-3} \left( \frac{1}{2} \ln(10) \right)^2 \sigma^2(2 \log(I)) \quad (3.6)$$

The next step is an amplifier that introduces the path length dependent coefficient of equation 3.4 as well as the factor  $10^{-12}$  in equation 3.2. The gain,  $G$ , of this amplifier is set with an external potentiometer (range 0 – 100k $\Omega$ ), which has a dial with a range from 0 to 1000. The gain is given by

$$G = \frac{5230 - 5.23P}{47 + P} . \quad (3.7)$$

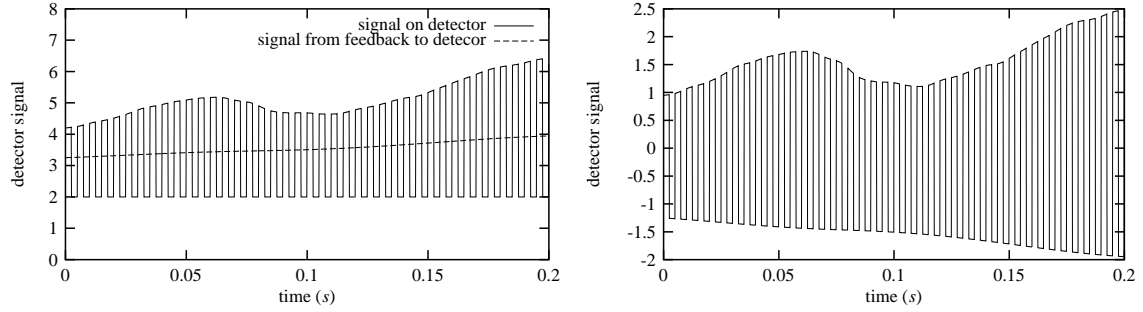


**Figure 3.1:** The effect of the feedback of the mean detector signal to the detector. The left graph shows the signal on the detector, as well as the mean level of the signal as it is determined by the feedback loop. The right graph shows the effect of the feedback loop: the absolute fluctuations (both from the turbulent signal and from the modulation) remain intact, but the offset due to ambient light is removed. Furthermore, the signal is shifted downward by half the mean distance between maximum and minimum of the transmitter signal. Note that the spectral separation between signal frequency and modulation frequency is an order of magnitude less in this example than in reality (the same holds for figure 3.2)

Equating this gain to the factor it should represent yields (remember that the gain is applied *before* the RMS computation and squaring):

$$\left(\frac{5230 - 5.23P}{47 + P}\right)^2 = 10^{12} \left(\frac{1}{2} \ln(10)\right)^2 1.12D^{7/3}L^{-3} . \quad (3.8)$$

This yields the following expression for the setting of the potentiometer<sup>1</sup>:

$$P = \frac{5230 - 47\frac{1}{2} \ln(10) \sqrt{10^{12} 1.12D^{7/3}L^{-3}}}{\frac{1}{2} \ln(10) \sqrt{10^{12} 1.12D^{7/3}L^{-3}} + 5.23} \quad (3.9)$$

The final step of the data processing is the determination of the variance of the signal. This is done with an RMS-to-DC converter with a dB output giving the logarithm of the RMS. The RMS-to-DC converter is calibrated such that the output is 2V per decade. Thus the output is:

$$\begin{aligned} V_{out} &= 2 \log(G\sigma(2 \log(I))) \\ &= \log(G^2\sigma^2(2 \log(I))) \\ &= \log(10^{12} 1.12D^{7/3}L^{-3}\sigma^2(\ln(I))) \\ &= \log(10^{12}C_n^2) \end{aligned} \quad (3.10)$$

### 3.2 Signal processing: electronics

The signal from the diode is converted in a number of steps. These steps are:

- a. The signal from the detector (which is supposed to vary linearly with the incident light intensity) is linearly amplified by two amplifiers, one internal in the detector, and one on a separate circuit board.
- b. In order to eliminate —slowly varying— natural light, the mean level of the signal is fed back to the detector. This results in an output signal which varies around a zero mean. The time constant of this feedback is of the order of 0.1 second (see also figure 3.1)<sup>2</sup>. The feedback signal thus varies with a

<sup>1</sup>This is equal to the equation used before:  $P = \frac{5476}{\sqrt{4.48D^{7/3}L^{-3}0.3314 \cdot 10^{12} + 5.23}} - 47$ .

<sup>2</sup>The figures have been made with artificial turbulent data (based on random data with an approximate -5/3 slope of the spectrum and a limited range of frequencies) The range of frequencies in the turbulent signal, the modulation frequency and the time constant of the feedback loop have been chosen such that the figures are as illustrative as possible. In reality, the spectral separation between modulation signal and the highest frequencies present in the turbulent signal will be at least an order of magnitude larger.

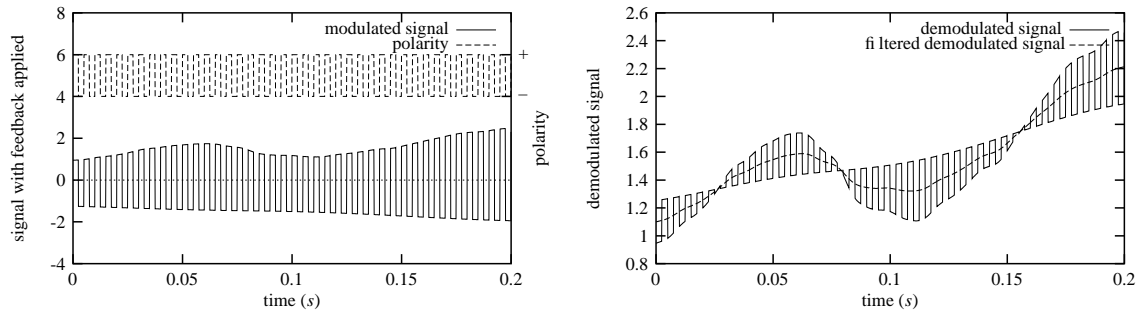


**Figure 3.2:** The demodulation of the detector signal: the polarity of the signal from the feedback circuit is switched based on the polarity of the signal itself. (the left graph shows the two constituents of this process). The result is a signal that follows the original signal as far as fluctuations are concerned that have a time scale longer than the time constant of the feedback circuit. Superimposed on this signal is a carrier signal with the same frequency as the original carrier signal. The carrier is modulated with the fluctuations that have a time scale which is shorter than that of the feedback signal. In order to remove all fluctuations due to the modulation (frequencies of the order of  $7000\text{kHz}$ ) the signal is low-pass filtered. This yields the original signal, with two differences: the mean value of the new signal is half that of the original signal and the amplitude of the new signal is half that of the original signal. All fluctuations with a time scale

frequency that is within the range of frequencies contained in the turbulent signal. The output signal of the detector is a block signal with a slowly varying minimum value and a maximum value that follows the turbulent signal.

- c. The signal (the output of step **b**) is demodulated in order to capture only the radiation coming from the LED of the transmitter (which is switched at  $7\text{kHz}$ ). Demodulation is done with *synchronous detection*: the polarity of the signal is switched based on the sign of the signal itself (in fact, this stage acts as a rectifier). The assumption in the use of this type of demodulation is that the actual signal (the value at times that the LED is switched on) does not contain zero-crossings. Figure 3.2 illustrates this process: the signal as well as the polarity are shown. The output of the demodulation step is shown in the left pane of figure 3.2. In order to remove the remains of the modulation-demodulation process, the resulting signal is passed through a low pass filter. It is important to note that the ratio of the amplitude of the fluctuations to the mean level is not affected by this scheme of feedback and demodulation. Furthermore, this example shows that the time constant of the feedback circuit is not important as far as the demodulation is concerned. It is important, however, in relation to the time scale of the fluctuations in the background radiation.
- d. The signal is low-pass filtered at  $400\text{Hz}$  to remove noise from the detector and high-frequency components left over from the demodulation step.
- e. The signal passes through a log-amplifier which converts the intensity fluctuations to log-intensity fluctuations. This amplifier is calibrated with two variable resistors. In fact, this amplifier has an output that is twice the  $^{10}\log$  of the input signal ( $2\text{V}$  per decade). The extra factor of two is absorbed in the path setting amplifier (see step **f**). The value of the input voltage of this log-amplifier is in the range of  $-1\text{ V}$  to  $-10\text{ mV}$  (depending on the signal strength; this voltage is in fact the demodulated signal). The corresponding range of output voltages is roughly  $-4\text{ V}$  to  $0\text{ V}$ .
- f. Then the signal is amplified with a gain that depends on the path length (variable), the wavelength of the light and the beam diameter (both constant). The conversion factor relates log-intensity variance to the structure parameter of the refractive index. The actual determination of the variance<sup>3</sup> is done at a later stage, but the signal can be multiplied with the conversion factor at any stage (after the first log-amplifier), since the factor is a constant. This conversion can be *set* with an external variable resistor.

<sup>3</sup>In the electronics the RMS value is determined rather than the variance, which results in an extra factor of 2 when taking the logarithm ( $\log x^2 = 2 \log x$ ).

The conversion is *calibrated* with a variable resistor in the electronics (this resistor determines the gain of an extra amplifier).

- g. The next step is a high-pass filter at  $0.1\text{Hz}$ . The low frequency cut-off is used to remove water vapour absorption fluctuations. Together with the low-pass filter (see **d**) this forms a bandpass filter.
- h. The signal again passes through a RMS-to-DC converter. Here the RMS is determined relative to an average signal which is a low-pass filtered version of the original signal. The time constant of the filter is 2.5 seconds (note that this is much less than the 0.1 second used in the feedback circuit (see step **b**)). The output of this RMS determination is a signal that is (apart from a constant shift of  $12\text{V}$ ) equal to  $\sqrt{C_n^2}$ . The RMS-to-DC converter possesses both a linear and a dB output. The latter is used in order to convert a signal that varies by orders of magnitude to a convenient output signal. Furthermore, the output signal is multiplied by 2 to remove the square root (output is  $2\text{V}$  per decade). Consequently, the signal at the dB output ( $V_{out}$ ) of the circuit is such that  $C_n^2 = 10^{V_{out}-12}$ . This log-amplifier is calibrated with two variable resistors. The input voltage of the log-amplifier is zero in the mean, and the amplitude is related to  $C_n^2$ : it ranges from 0 to roughly  $\sqrt{2}\text{V}$  (the output voltage of the amplifier ranges from  $-5$  to  $0\text{V}$ ; at an output voltage of  $0\text{V}$ , the RMS is  $1\text{V}$ , which corresponds roughly to an amplitude of  $\sqrt{2}\text{V}$  when a sinoid signal is assumed).
- i. Finally, the signal is fed to the internal data logger. The analog-to-digital converters of this data logger need to be calibrated.

### 3.3 Calibration of log-amplifiers in receiver

#### 3.3.1 Calibration procedure

Steps **e** and **h** involve the calibration of log-amplifiers. For each of the amplifiers two adjustable resistors are available for calibration<sup>4</sup>. One sets the gain and the other sets the offset of the amplifier. Both amplifiers should be calibrated such, that the output is  $-2\text{V}$  per decade (see Heusinkveld and Nieveen, 1997). First a reference voltage,  $V_{ref}$ , of  $1.000\text{V}$  is applied and the offset is set such that the output voltage is  $0.000\text{V}$ . This can be achieved within an accuracy of  $5\text{mV}$  or better (typically  $2.5\text{mV}$ ). Subsequently, the reference voltage is set to  $0.100\text{V}$  and the gain is adjusted in order for the output voltage to be  $-2.000\text{V}$ . This setting can also be achieved with an accuracy of better than  $5\text{mV}$ .

#### 3.3.2 Error estimate

In order to determine the maximum error due to inaccuracies in the log-amplifier calibration, it is assumed that the setting with  $V_{ref} = 1.000\text{V}$  has a deviation from its nominal value ( $0.000\text{V}$ ) with a sign opposite to the deviation at  $V_{ref} = 0.100\text{V}$ . Then the gain of the amplifier will be wrong by  $0.5\%$  ( $-2.01\text{V}$  per decade or,  $-1.99\text{V}$  per decade, depending on the sign of the deviations). The errors quoted here are the maximum errors. Besides, errors in gain and offset will compensate (since the setting of the offset is used in the calibration of the gain). Thus it is safe to assume that typical errors in the offset will be  $0.0025\text{V}$  and the error in the gain will be typically  $0.25\%$ .

The effect of possible errors in the log-amplifier calibration is different for the two amplifiers. The setting of the offset of the first amplifier is unimportant, since the resulting signal is used for an RMS calculation (which removes any error in the mean value). The error in the gain results directly in an error in the standard deviation of the log-intensity (which is determined in step **h**). The relative error in  $\sigma_{\ln(I)}$ , or equivalently  $\sqrt{C_n^2}$ , will be as large as the relative error in the gain setting of the first amplifier (of the order of  $0.25\%$ ). The error in  $\sigma_{\ln(I)}^2$  (or  $C_n^2$ ) will be twice that value.

Errors in the calibration of the second log-amplifier result in an error in the number that is used to store

<sup>4</sup>The circuitry around the log-amplifier contains a temperature dependent resistor that compensates for the temperature dependence of the output of the dB-output of the amplifier. For an accurate calibration, the receiver should be switched on for some time in order for the electronics to come in thermal equilibrium.

source of error	size of error	Error in $C_{n^2}$	
		at $V_{out} = -2V$	at $V_{out} = -4V$
offset amplifier 1	0.0025V	0	0
gain amplifier 1	0.25%	0.5%	0.5%
offset amplifier 2	0.0025V	0.6%	0.6%
gain amplifier 2	0.25%	1.2%	2.3%

**Table 3.1:** The effect of errors in the calibration of the two log-amplifiers on the derived value of  $C_{n^2}$ .

$C_{n^2}$  ( $C_{n^2} = 10^{V_{out}-12}$ ). Since it is  $C_{n^2}$  one is interested in, the error should be determined as:

$$\begin{aligned}
 \frac{\partial C_{n^2}}{\partial V_{out}} &= \frac{\partial 10^{V_{out}-12}}{\partial V_{out}} \\
 &= \ln 10 \cdot 10^{V_{out}-12} \\
 &= \ln 10 \cdot C_{n^2} .
 \end{aligned} \tag{3.11}$$

Thus the relative error in  $C_{n^2}$  is  $2.303\delta V_{out}$ , where  $\delta V_{out}$  is the absolute error in  $V_{out}$ . A miscalibration of the offset of the second log-amplifier of 0.0025V will result in a relative error in  $C_{n^2}$  of 0.6%. A relative error in the gain of 0.25%, at a value of  $V_{out} = -2V$  will result in an error of 5 mV in  $V_{out}$  and a relative error in  $C_{n^2}$  of  $\ln(10)0.005 = 1.2\%$ . Table 3.1 summarizes the results of this section.

## 3.4 Path setting on receiver

### 3.4.1 Calibration procedure

For the calibration of the path setting an artificial signal is used with a carrier frequency of  $7kHz$ , which is amplitude modulated with a block signal with a frequency of 20 Hz and a ratio between the high ( $H$ ) and low ( $L$ ) value of 2. This signal is fed directly to the demodulator unit. The RMS of the logarithm of this signal is  $\frac{1}{2} \log \frac{H}{L}$  and the resulting value of  $V_{out}$  will be  $2 \log(G \log(\frac{H}{L}))$  (see equation 3.10). In the calibration procedure the gain is set such that  $V_{out} = 0$ , or  $G = (\log(\frac{H}{L}))^{-1}$ . The corresponding setting of the potentiometer is:

$$P = \frac{5230 \log(\frac{H}{L}) - 47}{1 + 5.23 \log(\frac{H}{L})} . \tag{3.12}$$

For the given ratio  $\frac{H}{L}$  of 2 this implies  $P = 593.3$  (corresponding to a path length of 1180 m) This setting of  $V_{out} = 0$  can be attained within 5mV. The setting of  $P$  can be made with an accuracy of  $\pm 1$  division<sup>5</sup> (total scale of dial is 1000).

### 3.4.2 Error estimate

In the path setting amplifier two sources of error determine the accuracy of the  $C_{n^2}$  signal: the finite accuracy of the potentiometer setting, and the finite accuracy of the calibration to  $V_{out} = 0V$ . For the moment the error due to errors in the signal used for the calibration is not taken into account.

$C_{n^2}$  is proportional to  $G^2$ , so the relative error in  $C_{n^2}$  due to an error in  $P$  ( $\delta P$ ) is:

$$\begin{aligned}
 \frac{1}{C_{n^2}} \frac{\partial C_{n^2}}{\partial P} &= \frac{1}{G^2} \frac{\partial G^2}{\partial P} \\
 &= 2 \frac{1}{G} \frac{\partial G}{\partial P} \\
 &= 2 \frac{47 + P}{5230 - 5.23P} \frac{-5476}{(47 + P)^2} .
 \end{aligned} \tag{3.13}$$

<sup>5</sup>This is an optimistic estimate.

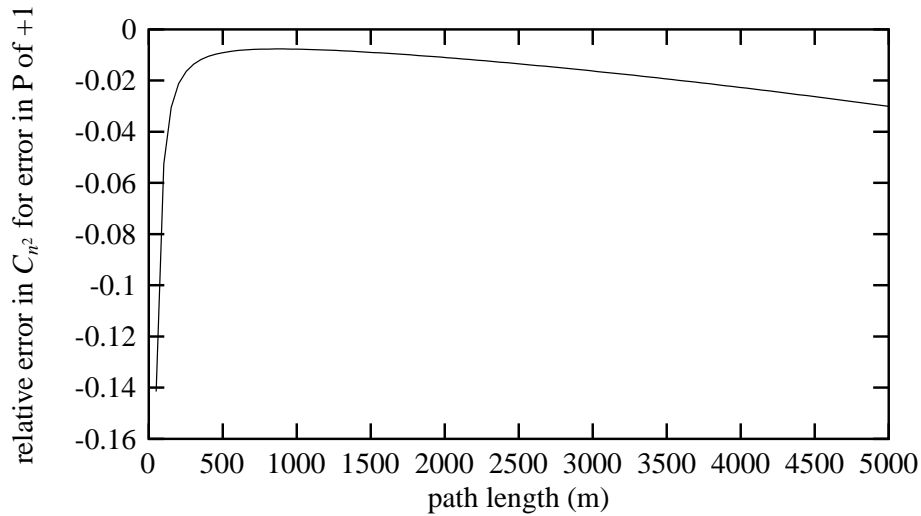


**Figure 3.3:** The relative error in  $C_{n^2}$  due to an error  $\delta P = 1$ .

source of error	size of error	Error in $C_{n^2}$		
		at $L = 1000m$	at $L = 2000m$	at $L = 5000m$
pot setting during calibration	1	0.8%	0.8%	0.8%
$V_{out}$ during calibration	0.0025V	0.6%	0.6%	0.6%
pot setting during measurement	1	0.8%	1.1%	3.0%

**Table 3.2:** The effect of errors in the calibration and setting of the path setting amplifier on the derived value of  $C_{n^2}$ . Numbers are valid for  $D = 0.152m$

The relative error in  $C_{n^2}$  due to an error  $\delta P = 1$  is shown in figure 3.3 as a function of the path length.

The sensitivity of  $C_{n^2}$  to  $P$  plays a role both during the calibration and during the measurements, due to the finite accuracy with which the external potentiometer can be set to a certain value. During the calibration incorrect pot setting will result in an incorrect setting of the gain of the extra amplifier, and thus a constant relative error in  $C_{n^2}$  during the measurements. An incorrect pot setting during the measurements will cause a relative error in  $C_{n^2}$  that depends on the sensitivity of  $C_{n^2}$  to at the given pot setting (or equivalently, path length). If during the calibration  $V_{out}$  is not set to 0V but to  $V_{err}$ , then the relative error in the gain setting will be  $10^{0.5V_{err}} - 1$  and the resulting error in  $C_{n^2}$  will be  $2(10^{0.5V_{err}} - 1)^6$ . Table 3.2 summarizes the relative errors in  $C_{n^2}$  due to errors in the path setting. The numbers quoted are valid for a beam diameter of 0.152m.

## 3.5 Calibration of internal data logger

In this section the contribution of the internal data logger to errors in the stored  $C_{n^2}$  is studied.

### 3.5.1 Procedure

The LAS is equipped with an internal data logger, Micro-G2 (Z-world Engineering Davis, CA.). See also Z-World (1996). The two channels of the data logger that are used in the LAS are both conditioned ADC's. The resolution of the ADC's is 4096 bits. The range of these ADC's is controlled by a pair of resistors (one for the gain, another for the offset). In the present situation resistors of 2.2 k $\Omega$  and 6.8 k $\Omega$  are used for

<sup>6</sup> $V_{err} = 2 \log(\log(\frac{H}{L})G_{err})$ , thus  $10^{0.5V_{err}} = G_{err} \log(\frac{H}{L})$  and  $10^{0.5V_{err}} = G_{err}/G$ . Consequently, the relative error in  $G$  equals  $G_{err}/G - 1 = 10^{0.5V_{err}} - 1$ . Since  $C_{n^2}$  is proportional to  $G^2$ , the relative error in  $C_{n^2}$  will be  $2(10^{0.5V_{err}} - 1)$ .



source of error	size of error	Error in $C_{n^2}$	
		at $V_{out} = -2V$	at $V_{out} = -4V$
calibration voltage: gain	0.02%	0.09%	0.2%
calibration voltage: offset	$\ll 1$ bit	0	0
discretization during calibration: gain	0.06%	0.3%	0.6%
discretization during calibration: offset	0.5 bit	0.3%	0.3%
discretization during measurement	0.5 bit	0.3%	0.3%

**Table 3.3:** The effect of errors in the calibration of the internal data logger on the derived value of  $C_{n^2}$ .

the gain and offset resistors, respectively. This results in a range of  $-5.75V$  to  $+5.61V$ . The ADC's of the internal data logger are calibrated with an external voltage calibrator (Time Electronics Ltd, DC Voltage calibrator, accuracy 0.02%<sup>7</sup>). Two voltages are applied, usually  $-2.5V$  and  $2.5V$ . From these, the gain and offset (V/bit and bits, resp.) are determined.

### 3.5.2 Error estimate

Three error sources can be identified in the step of converting the LAS output voltage  $V_{out}$  to a binary number:

- Finite accuracy of the voltage source;
- Discretization error during calibration;
- Discretization error during measurement;

The error in the calibration voltage fed to the data logger will be 0.02% times  $2.5V$  equals  $0.5 mV$ . This results in an error of the offset of much less than one bit (since the resolution is  $2.77 mV/bit$ ). The error in the gain is 0.02% (assuming the errors in the two calibration voltages to have opposite signs).

The error in the recorded voltage due to the discretization of the ADC is 0.5 times the resolution:  $1.4 mV$ . This is also the error in the calibrated offset. The error in the gain is 0.06% (assuming the discretization error to be of opposite sign for the two calibration voltages).

The effects of the different error sources on  $C_{n^2}$  is summarized in table 3.3. It can be concluded that even when all errors linked to the ADC calibration occur at once, the error in the estimated  $C_{n^2}$  is 1% or less.

## 3.6 Error sources not addressed here

A number of error sources can be identified that have not been dealt with in the previous sections. These include:

- Drift of the two log-amplifiers, the path-setting amplifier or the data logger calibration.
  - An example of the magnitude of the drift of the log-amplifiers is shown in figure 3.4; one can see that for the regions of interest ( $-5 < V < 0$ ) the deviation due to drift is at most 20 mV. This is about twice the inaccuracies in the calibration.
  - The drift of the path-setting can be seen in figure 3.6. Again the drift is of the order of twice the inaccuracy in the calibration.
- Non-linearity of the two log-amplifiers, the path-setting amplifier or the data logger calibration.
  - Figure 3.5 shows an example of the non-linearity of the two log-amplifiers of a new LAS. For the first log-amplifier the error in the signal processing will be largest at low signals strengths (low 'demod' signal). The non-linearity in the second log-amplifier will only affect signals with a low  $C_{n^2}$ . The absolute error in  $C_{n^2}$  will be low then.

<sup>7</sup>It is not completely clear whether this 0.02% of the full scale range, or 0.02% of the actual value. The latter will be assumed.

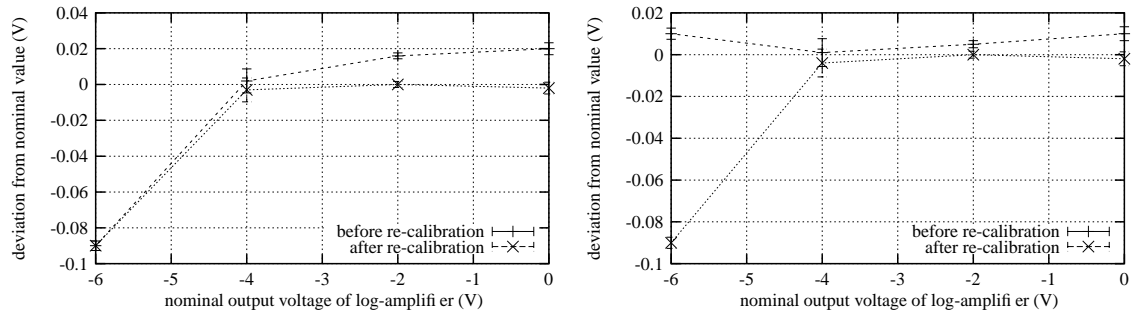


**Figure 3.4:** An example of the drift of the log-amplifier: first (left) and second (right) log-amplifier from LAS 98002. One line shows the deviation from the nominal output voltage of the amplifier before re-calibration. The other line shows the deviations after re-calibration. The error shown comprises errors inherent to the calibration itself (see table 3.1), the finite accuracy of the voltage calibrator and the finite resolution of the voltmeter used obtained the current data. Before the re-calibration, the LAS had been in the field in Turkey for several months.

- Figure 3.6 gives an indication of the non-linearity in the path-setting amplifier. It should be noted, however, that this graph shows the effect of the total electronics (from detector to  $V_{out}$ ) rather than the path-setting only. After recalibration the errors are within the limits of errors due to external uncertainties.

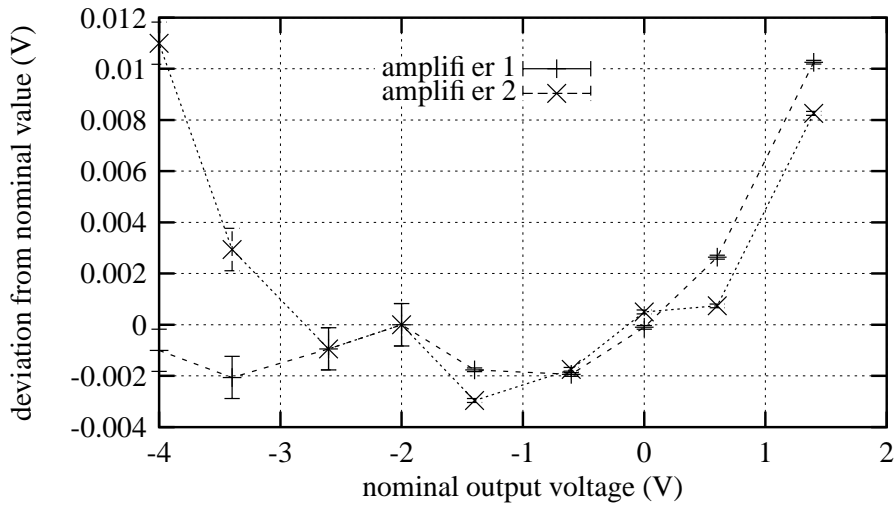


**Figure 3.5:** An example of the non-linearity of the log-amplifiers: first and second log-amplifier from LAS 99005 after calibration. Shown is the deviation from the nominal output voltage from the amplifier as a function of the nominal value. The error shown comprises the finite accuracy of the voltage calibrator and the finite resolution of the voltmeter used obtained the current data (the error inherent to the calibration (table 3.1) is irrelevant here). At the time of this calibration the LAS was new.

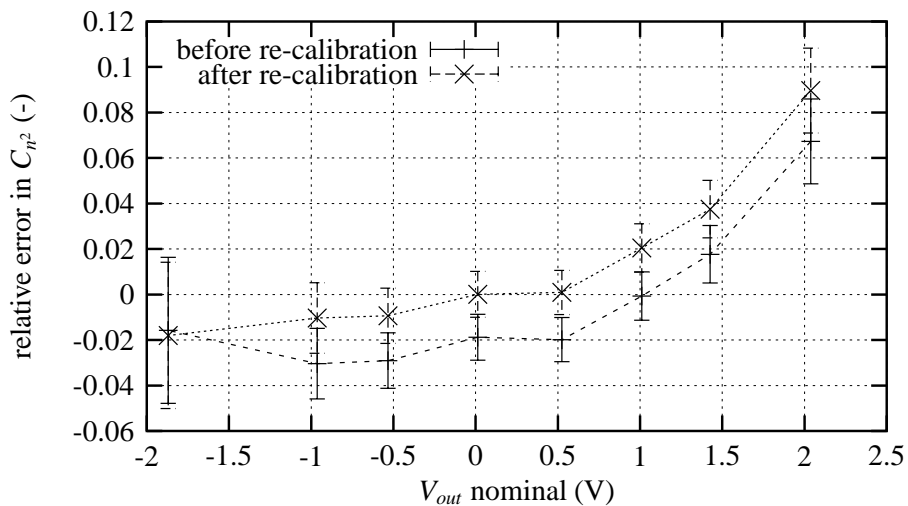


**Figure 3.6:** An example of the drift of the path-setting amplifier. The relative error in  $C_p^2$  is shown as a function of the nominal value of  $V_{out}$ . The data have been generated as follows: modulated signal is fed into the electronics (to mimic an actual detector signal). The modulation depth of this signal is such that it gives  $V_{out} = 0$  at a path setting of 1184 m. The path setting is varied to give a range of values of  $V_{out}$ . Note that  $V_{out} > 0$  is outside of the normal operational range. The error bars include all errors listed in table 3.2. The LAS used is LAS 98001. Recalibration was done after the LAS had been in Turkey for some months.

---

# Bibliography

Heusinkveld B. and Nieveen J. (1997). Large aperture scintillometer - user manual and technical information. unpublished.

Jenkins F. and White H. (1976). *Fundamentals of optics*. McGraw-Hill, New York, etc., 4th edn.

Wang T., Ochs G. and Clifford S. (1978). A saturation-resistant optical scintillometer to measure  $C_n^2$ . *J. Opt. Soc. Am.*, 68, 334–338.

Z-World (1996). *Micro-G2. C-programmable Miniature Controller. Technical Reference Manual*. Z-World Engineering, 12724 Picasso Avenue, Davis, CA 95616.